Micromechanical Velcro

Hongtao Han, *Student Member, IEEE*, Lee E. Weiss, *Member, IEEE*, and Michael L. Reed, *Member, IEEE*

***Abstract*—We have developed arrays of micromechanical mating structures, fabricated with silicon micromachining techniques, which act as mechanical adhesives. The microstructures are fabricated on standard silicon wafers, with an areal density of approximately 200 000 per cm². The microstructures on two identical surfaces will self-align and interlock with each other under application of adequate external pressure. A tensile strength per unit interlocked area of 1.1 MPa, or 160 psi, has been achieved. In this paper, we describe the design and fabrication of this "micromechanical Velcro"; we also present results of our experimental tests, a theoretical estimate of the tensile strength, and design constraints.**

Introduction

We have applied silicon micromachining technology to fabricate dense regular arrays of microstructures which act as surface adhesives. The principle of bonding is that of a button snap, or a zipper, but in a two-dimensional configuration. The bonding principle is depicted by the schematic cross section in Fig. 1. When two surfaces fabricated with identical microstructures are placed in contact, the structures self-align and mate. Under application of adequate external pressure, the tabs of the structures deform and spring back, resulting in an interlocking of the two surfaces. The interlocking bond is reminiscent of Velcro™; however, unlike Velcro, a permanent bond is achieved.

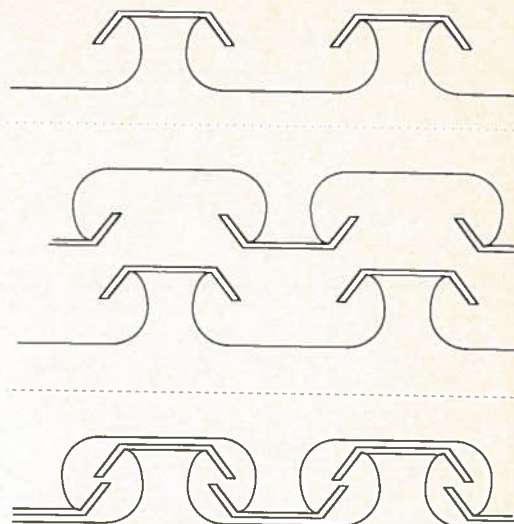

Fig. 1. Top: schematic cross section of the micromechanical structures. Center: when mating structures are pressed together, the tabs deform and spring back. Bottom: interlocked microstructures.

An electron micrograph of the microstructures is shown in Fig. 2. Minimum loads of approximately 12 kPa are necessary to bond the two substrates together. Tensile strength of the bond is in excess of 240 kPa. We have verified that the bonding is due to interlocking by a variety of techniques, including direct examination in an electron microscope.

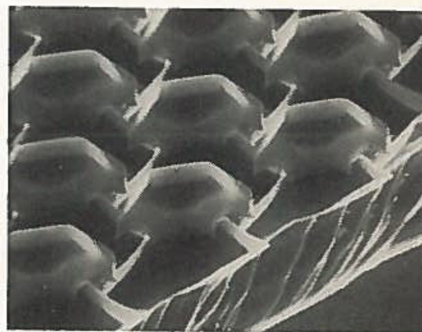

Fig. 2. Electron micrograph of micromechanical fastening structures.

Several applications for this technology are under development. Advantages over conventional adhesives include thermal tolerance, resistance to chemical attack, and self-alignment. Sharp, pointed microstructures, which will bond to biological tissues, can also be fabricated [1]; these are useful for medical applications.

In the following sections, we will describe the fabrication process, mechanical testing, estimated theoretical strength, and design contraints for the microstructure arrays.

Manuscript received August 14, 1991; revised October 23, 1991. Subject Editor K. Petersen. This work was supported by the National Science Foundation.

H. Han and M. L. Reed are with the Department of Electrical and Computer Engineering, Carnegie Mellon University, Pittsburgh, PA 15213-3890.

L. E. Weiss is with the Robotics Institute, Carnegie Mellon University, Pittsburgh, PA 15213-3890.

IEEE Log Number 9105429.

™Velcro is a trademark of Velcro USA, Manchester, NH.

Fabrication Process

Fig. 3 illustrates the process sequence [2]. A 1200 Å SiO_2 layer is grown at 1000°C in dry oxygen on (100) silicon wafers. The oxide is patterned into an array of 10 μm square islands, with one edge aligned 45° to the (110) flat. After photoresist stripping, the wafer is immersed into an anisotropic etch bath consisting of aqueous KOH (33–45%, 84°C, 4 min) and isopropyl alcohol. The etching results in a truncated pyramid or frustrum with exposed (212) planes, which are the fastest etching surfaces

1057-7157/92$03.00 © 1992 IEEE

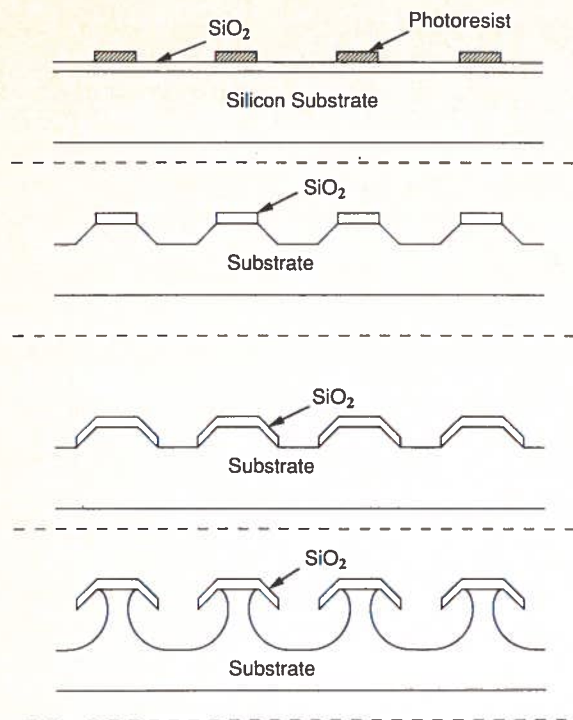

Fig. 3. Microstructure fabrication process. The caps are 1.0 μm of SiO_2 atop silicon pedestals.

[3]. The (212) planes intercept the (100) base plane at an angle of 48°.

After stripping the masking oxide, and cleaning the samples with a conventional chemical sequence, a thick SiO_2 film, about 1.0–1.5 μm, is grown at 1000°C in wet oxygen. The oxide is patterned by a second mask consisting of an array of Greek crosses, each approximately 18 μm wide, aligned to the original array. The SiO_2 crosses act as a mask for a second etch in KOH ($\approx$3 min) which removes some of the underlying silicon. Finally, the microstructures are completed by etching the wafer in an isotropic etching bath (15:5:1 HNO_3 : CH_3COOH : HF, 2 min). This step provides the vertical clearance for the interlocking mating structures, and the lateral undercut necessary to produce the four overhanging arms. Although the isotropic silicon etch also attacks SiO_2, the selectivity is sufficiently large as to not erode the SiO_2 caps significantly.

The second masking step poses particular difficulties, since the surface is highly nonplanar after the first mask. We have successfully patterned the wafers by using a nominal 2.1 μm thick photoresist film, combined with a long exposure time. The resist thickness, as measured from electron micrographs, is highly nonuniform; it reaches about 3.0 μm in the field regions, and is severely thinned over the tops of the frustums. However, there is adequate thickness to prevent the buffered HF etchant from attacking the SiO_2 caps.

The isotropic silicon etch after the second masking step results in considerable lateral undercutting. To prevent this encroachment from weakening the silicon pedestals supporting the SiO_2 caps, we use two techniques: 1) the inside corners of the Greek cross mask pattern are filleted to reduce the undercutting; and 2) the isotropic etch is preceded by an anisotropic etch in KOH, as described above. This step reduces the undercutting by supplying most of the needed vertical clearance, without compromising the integrity of the silicon support.

Although the microstructures themselves are tiny, useful bonding strengths are realized when macroscopic scale arrays are utilized. Our present design uses a pitch of 22 μm, which results in an areal density of over 200 000 microstructures per square centimeter. An important factor in the array alignment is the runout error in the mask set; field stitching errors must be held to a minimum to maintain the array regularity.

Mechanical Testing

The bond strength of the mating structures was characterized by direct measurements of the tensile load needed to induce failure. Patterned samples, nominally 8 mm × 8 mm, were mounted on glass microscope slides using cyanoacrylate adhesive. The mating surfaces were placed together in rough angular alignment, as observed with a low power microscope. Slight shaking of the samples was sufficient to precisely align the microstructures into a mating position. Interlocking was accomplished by applying a load to the upper substrate; the pressure was monitored by placing the entire assembly on an electronic force scale. Bonding was considered to have taken place once the weight of the lower sample and glass slide could be supported by the upper sample. The minimum load necessary for interlocking corresponds to a pressure of 12 kPa. (This compares to a value of 7×10^5 kPa which is needed to crush the silicon wafers.)

Bond strength was determined by applying a tensile load through a pulley and measuring the force necessary for separation. We find that separation of the samples is always accompanied by damaged areas on corresponding regions of the mating surfaces. Close-ups of the microstructures in these areas reveal fracturing of the SiO_2 tabs near the juncture with the silicon support post. We interpret this as evidence the samples are interlocking only over the damaged region. Furthermore, the fraction of damaged area is proportional to the initial loading. For example, a loading of 110 kPa results in an interlocked area of 13%; increasing the insertion load to 330 kPa causes 21% of the microstructures to latch. Fig. 4 shows the relationship between the interlocked area and the insertion pressure, as well as the dependence of tensile strength on the fraction of latched area. In addition to insufficient loading, partial interlocking could also be caused by particulate contamination which prevents uniform loading of the samples.

Taking the ratio of applied load to the sample area, we observe tensile strengths on the order of 10–250 kPa. However, if these values are corrected by the fraction of interlocked area, as estimated from the pattern of damage

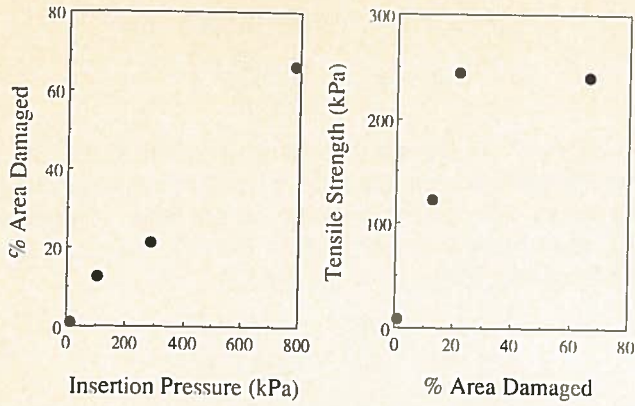

Fig. 4. Measurements of interlocked area (left) and tensile strength (right) with increasing insertion pressure.

Fig. 5. Electron micrograph of mated structures (top-down view along edge).

after separation, the tensile strength per unit of interlocked area is higher, about 400–1100 kPa. The first three data points in Fig. 4 show a linear increase in tensile strength as the fraction of latched area increases. The extrapolated value of tensile strength is 1100 kPa, which is in approximate agreement with the calculated strength at 100% latching, as described in the next section. The remaining data point does not fall on this curve. We do not fully understand the reason for this. One possibility is that the microstructures on this sample broke upon insertion, so that the damaged area is not representative of the latched fraction. It is also possible that our calculations are in error and for some reason the tensile strength saturates at approximately 250 kPa. We are currently investigating the behavior of the fastening system at higher insertion pressures to understand this problem.

It is well known that silicon wafers placed in intimate contact will bond to each other, especially if moisture is present [4]–[7]. To distinguish this phenomenon from the latching mechanism, we repeated our measurements with wafers without the arrays of microstructures. Depending on the surface treatment (native oxide, thermal oxide, HF-dipped) and the relative humidity (38–100%), the tensile strength of the bonded pairs varied from 12 to 20 kPa, well below the strength of the patterned samples. Similar results were obtained when the microstructure arrays were grossly misaligned. Fig. 5 shows two interlocked samples, as viewed from above the edge of the upper sample. Close examination of this and other regions confirms that the bonding is indeed due to latching of the microstructure tabs.

Analysis

Failure Mechanisms

To separate two interlocked surfaces, sufficient force has to be applied. We take the externally applied tensile force per unit area required to separate the two bonded surfaces as a measure of the bonding strength of the microstructures.

As an approximation, we can use a simple cantilevered beam picture to model the forces on the microstructures [1], [8]–[10]. Fig. 6 diagrams the forces acting during separation of the two bonded surfaces. P_n is the interaction force between two tabs acting at the ends of the tabs; l represents the length of the tabs, and α is the angle between P_n and the substrate plane. Because the applied force acts as a transverse load on the beams, both bending and shearing stresses exist in the tabs. Below, we calculate which of these two stresses is dominant in the failure of the microstructure tabs.

The bending stress, σ, is related to the bending moment $M(x) = P_n(l - x)$ by the flexure formula:

$$\sigma_x = \frac{M(x)y}{I_z} \tag{1}$$

where I_z is the moment of inertia of the cross-sectional area about the centroidal axis, which is equal to $bh^3/12$ for a rectangular cross section beam of width b and thickness h, and y represents the distance from the neutral plane. The maximum bending stress $\sigma_{\max}$, which occurs on the upper and lower edges at the fixed corners of the tabs, i.e., $x = 0$, $y = \pm h/2$, can be expressed by

$$\sigma_{\max} = \frac{6P_n l}{bh^2}. \tag{2}$$

When this maximum bending stress reaches the yield point stress of the material σ_{yp}, the tabs of the structure will break at the fixed corners.

We can also calculate the magnitude of the shearing stress arising from the transverse load. Again, treating the tabs like a cantilevered beam, the resulting shearing stress τ_{xy} is given by [9]

$$\tau_{xy} = \tau_{yx} = \frac{P_n}{2I_z}[(h/2)^2 - y^2]. \tag{3}$$

We see that the shearing stresses are not uniformly distributed from top to bottom in the beam. The maximum value of τ_{xy} occurs at $y = 0$, i.e., for points on the neutral

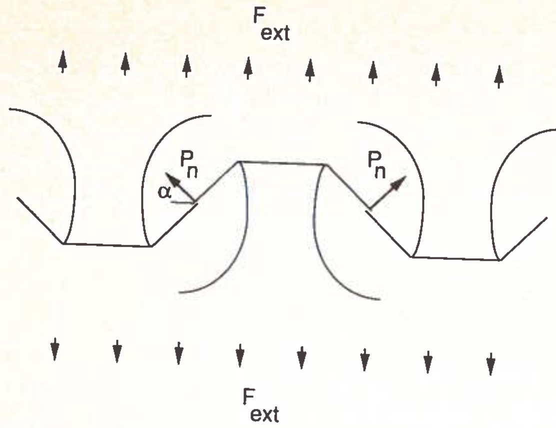

Fig. 6. Force diagram during separation of microstructures.

plane. This maximum stress is given by

$$\tau_{\max} = \frac{3P_n}{2bh}. \tag{4}$$

When $\tau_{\max}$ reaches the material's yield point value, the beams will collapse, starting at the neutral plane.

Experimentally, we observe failures consistent with the bending stress mechanism, and not the shearing stress failure mode. One can compare the expressions for $\sigma_{\max}$ and $\tau_{\max}$:

$$\frac{\tau_{\max}}{\sigma_{\max}} = \frac{h}{4l}. \tag{5}$$

For our design, $h/l \sim 1/7.5$, therefore,

$$\frac{\tau_{\max}}{\sigma_{\max}} \sim \frac{1}{30}. \tag{6}$$

Thus, the bending stress is about 30 times larger than the shearing stress, confirming the experimental observation that the tabs always break at the corners when the substrates are separated.

Another possible failure mechanism is breakage of the silicon pedestal supporting the tabs. Properly designed, the microstructures will fail by breaking at the fixed corners of the tabs as described above. We were able to induce failures of the silicon pedestal by intentionally increasing the lateral undercut during the isotropic silicon etch. In these cases, the pedestals necked down, weakening them sufficiently to fail when tensile force was applied. However, only by deliberately overetching the pedestal was this failure mode observed; the lateral undercut obtained in normal processing produced pedestals which would never fail before the tabs.

Estimate of Tensile Strength

For simplicity, we consider a one-dimensional cantilevered beam model, where the coupling between the four tabs of the Greek cross is neglected. Ignoring frictional forces, an applied external tensile force F_{ext} (per unit area) results in a force on each microstructure beam of

$$P_n = \frac{F_{ext} d^2}{4 \sin \alpha} \tag{7}$$

where $4/d^2$ is the areal density of cantilevered beams (four beams on each structure, placed in a square array d cm apart). The maximum stress in the beam is given by (2), and occurs at points furthest from the neutral axis of the fixed end, at $(x, y) = (0, \pm h/2)$:

$$\sigma_{\max} = \frac{6P_n l}{bh^2} = \frac{3F_{ext} d^2 l}{2bh^2 \sin \alpha}. \tag{8}$$

When this stress reaches the yield point stress of the tab material, σ_{yp}, the beam will break. Setting $\sigma_{\max}$ equal to the yield point stress, we can rearrange this equation to show the applied external force describing the bonding strength:

$$F_{ext} = \frac{2\sigma_{yp} bh^2 \sin \alpha}{3d^2 l}. \tag{9}$$

If friction between the interlocked tabs is taken into account, the above equation is modified by a term representing the frictional force contribution:

$$F_{ext} = \frac{2\sigma_{yp} bh^2 \sin \alpha}{3d^2 l} (1 + \mu \cot \alpha) \tag{10}$$

where μ is the coefficient of static friction.

Substituting our design values into the above equation, ($b = 10$ μm, $h = 1$ μm, $l = 7.5$ μm, $\alpha = 42°$, $d = 22$ μm) and taking $\mu = 0.5$ and $\sigma_{yp} = 6.0 \times 10^5$ kPa [11], yields a tensile strength of $F_{ext} = 1.1$ MPa. This value is at the upper end of the range of our present experimental measurements.

Although the simple cantilevered beam model cannot yield highly accurate values of the microstructure mechanical properties, it does give an easily understood and explicit physical picture of the important design parameters and trends. This model is thus useful for estimating the strength of a given microstructure design. A more rigorous calculation would include other effects, such as the coupling between tabs, the weight of the tabs, and a short beam correction. Qualitatively, the coupling between tabs will change the stress and bending moment distribution as to increase the strength of the microstructures.

Stored Strain Energy

Two surfaces bonded together generally separate by crack propagation. The strength of the bond can be quantified by the magnitude of the energy associated with the surface. There exists a way to relate the surface energy and the fracture length [12], but there is no satisfactory method of relating the surface energy to the tensile strength.

However, this limitation does not apply for the microstructure arrays, since the failure mode is not a fracture mechanism, but a more macroscopic yielding behavior.

Therefore, the energy associated with the bond can be calculated by determining the work required to strain the array of cantilevers into yielding. This work represents the stored strain energy in the SiO_2 beams just before they break. This calculation is useful because it provides a way to compare the bond strength of the micromechanical fastening system with other surface bonding technologies.

From elementary beam theory, the strain energy stored in the deflected beam by bending, ignoring the shearing stress, can be expressed by [10]

$$U = \int_0^l \frac{M(x)^2\,dx}{2EI_z} \tag{11}$$

where U is strain energy stored in a single deflected cantilevered beam, and E is Young's modulus of the material. For $M(x) = P_n(l - x)$, we have

$$U = \frac{P_n^2 l^3}{6EI_z}. \tag{12}$$

Using (8), U can also be expressed in terms of $\sigma_{\max}$ as

$$U = \frac{1}{9}(bhl)\frac{\sigma_{\max}^2}{2E}. \tag{13}$$

Accordingly, the "surface energy," which represents the total energy stored in the deflected beams per unit area, is equal to

$$U_s = \frac{4}{d^2}U \tag{14}$$

i.e.,

$$U_s = \frac{2}{9}\frac{bhl}{d^2}\frac{\sigma_{\max}^2}{E}. \tag{15}$$

At the yield point, $\sigma_{\max} = 6.0 \times 10^8$ Pa (the yield point strength of SiO_2), $E = 8.3 \times 10^{10}$ Pa [11], [13], and taking $h = 1.5$ μm, $l = 5$ μm, $b = 6.2$ μm, $d = 17.5$ μm (see the following section), then U_s is equal to 146 mJ/m^2, which is about twice as large as the bonding energy for hydrophilically bonded wafers [5], [6].

This calculation assumes that the bond failure is associated with the simultaneous failure of all the microstructures. This is, of course, an idealization; a chain is only as strong as its weakest link. Nonuniform interlocking will result in a torque, as well as a tensile load, which would result in sequential, not simultaneous, microstructure yielding. This has the effect of lowering the apparent bond strength.

Design Rules

Equation (10) describes the dependence of the tensile strength on several parameters: material properties, static friction, microstructure spacing d, cap thickness h, and tab length and width l and b. (Fig. 7 illustrates the geometrical parameters of the microstructures.) However, the geometrical parameters are not independent, since the tabs must be long enough to interlock. An attempt to increase the strength by increasing the areal density of microstructures will be offset by the decrease in tab width b. One can optimize the design of the microstructures, and predict the tensile strength by using (10) as a guide. The geometric requirement for interlocking can be expressed as

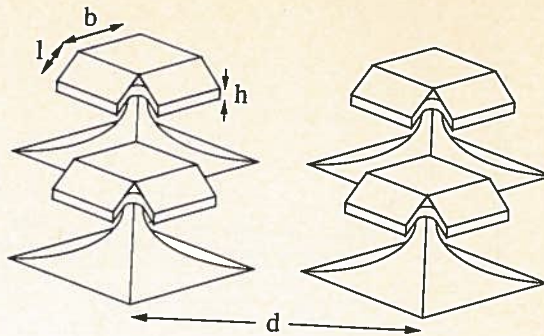

Fig. 7. Geometrical design parameters for the interlocking microstructures.

$$d = \sqrt{2}(2l \sin\alpha + b - \delta) \tag{16}$$

where δ is the projected overlap between the interlocked tabs when two surfaces are mechanically bonded together. Substituting this expression in (10), we obtain

$$F_{\text{ext}} = \frac{\sigma_{yp} h^2 \sin\alpha(1 + \mu\cot\alpha)}{3lb\left(1 + \dfrac{2l\sin\alpha - \delta}{b}\right)^2}. \tag{17}$$

We examine each parameter to see how a high tensile strength, F_{ext}, can be achieved.

1) Tab Thickness, h: Because F_{ext} increases as h^2, a thicker tab will greatly increase the tensile strength. The tradeoff is that the initial loading force also increases, which puts tighter limits on the acceptable range of overlap δ. Another difficulty is the larger vertical clearance needed, which increases the lateral undercut and can thus weaken the silicon pedestal. A range of $1.0\ \mu\text{m} < h < 1.5\ \mu\text{m}$ gives satisfactory performance.

2) Tab Length, l: The tab length l should be as small as possible; this allows a higher density of microstructures in the array, and produces stronger tabs. The practical lower limit is set by the lithographic tools; the variance in overlap δ must be small compared to the tab length for reproducibility. This sets a lower limit on l of about 5 μm.

3) Tab Width, b: An optimum value of b can be found by setting to zero the derivative of (17) with respect to b. Given a value for l and δ, the optimum value of b to maximize the tensile strength is found to be $b = 2l \sin\alpha - \delta$.

4) α, σ_{yp}, and μ: Angle α is determined by the etching properties of the substrate. If another fabrication process were used, this could possibly be controlled, but the effect on F_{ext} would be small. σ_{yp} and μ are materials related; μ also depends on the condition of the tab surfaces. Clearly, one could use a material such as silicon nitride or chro-

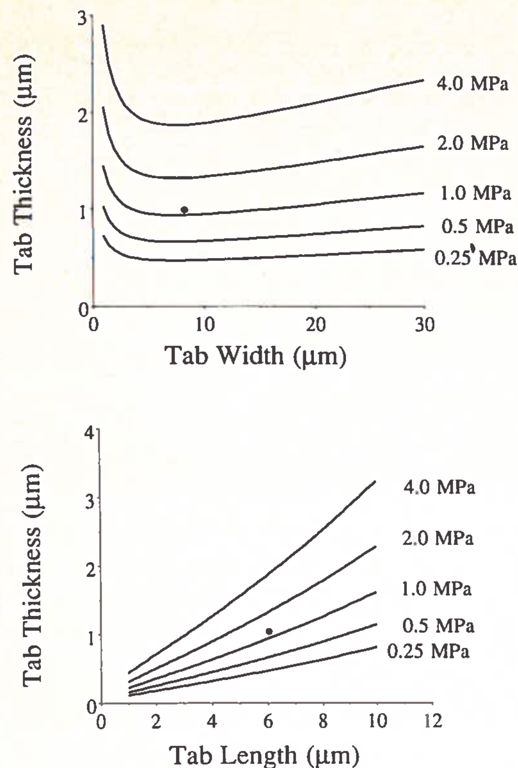

Fig. 8. Curves of constant tensile strength. Top: tab thickness versus width ($l = 6$ μm). Bottom: tab thickness versus length ($b = 8$ μm).

mium with a larger yield point strength to increase the tensile strength of the bond.

Fig. 8 shows curves of constant tensile strength curves for various combinations of the geometric parameters. The dot illustrates the design parameters for the experimentally tested arrays.

We can estimate what the maximum useful strength of this micromechanical Velcro would be if the design were optimized. Sticking to SiO_2 for the tabs, we can choose an optimum design with the following parameters: $l = 5$ μm, $\delta = 0.5$ μm, $\alpha = 42°$, $b = 2l \sin\alpha - \delta = 6.19$ μm, $h = 1.5$ μm, $d = 17.5$ μm. This gives an estimated tensile strength of $F_{ext} = 3.54$ MPa, for $\mu = 0$; with $\mu = 0.5$, $F_{ext} = 5.51$ MPa, or almost 800 psi. Silicon nitride or chromium tabs would increase the tensile strength by a factor of two or three.

Summary

We have described a micromechanical fastening system, based on silicon micromachining technology, which results in a strong, permanent bond without chemical adhesives. Since the bonding mechanism is purely mechanical, it can be used in applications where chemical resistance, thermal tolerance, and/or biological compatibility are paramount. Successful demonstration of the bonding principle has been achieved for this new micromechanical surface adhesive. Calculations of the tensile strength are in approximate agreement with the experimental results. Design rules have been developed which predict bond strengths as high as 5.5 MPa could be achieved by optimizing the geometry of the microstructures.

Acknowledgment

The authors wish to thank M. Wholey, C. Bowman, L. Rathbun, T. Schlesinger, W. Maly, P. Steif, and K. Hartmann for their assistance. Mask fabrication was performed at the National Nanofabrication Facility at Cornell University.

References

[1] H. Han, L. E. Weiss, and M. L. Reed, "Mating and piercing micromechanical structures for surface bonding applications," in *IEEE Workshop Micro Electro Mech. Syst.* (MEMS-91), Nara, Japan, 1991, pp. 253-258.

[2] H. Han, M. L. Reed, and L. E. Weiss, "A mechanical surface adhesive using micromachined silicon structures," *J. Micromechanics and Microeng.*, vol. 1, no. 1, pp. 30-33, 1991.

[3] X. Wu and W. H. Ko, "Compensating corner undercutting in anisotropic etching of (100) silicon," *Sensors and Actuators*, vol. 18, pp. 207-215, 1989.

[4] J. Haisma, G. A. C. M. Spierings, U. K. P. Biermann, and J. A. Pals, "Silicon-on-insulator wafer bonding-wafer thinning technological evaluations," *Japan J. Appl. Phys.*, vol. 28, no. 8, pp. 1426-1443, 1989.

[5] V. Lehmann, U. Gosele, and K. Mitani, "Contamination protection of semiconductor surfaces by wafer bonding," *Solid State Technol.*, vol. 33, no. 4, pp. 91-92, 1990.

[6] W. P. Maszara, G. Goetz, A. Caviglia, and J. B. McKitterick, "Bonding of silicon wafers for silicon-on-insulator," *J. Appl. Phys.*, vol. 64, no. 10, pp. 4943-4950, 1988.

[7] J. B. Lasky, "Wafer bonding for silicon-on-insulator technologies," *Appl. Phys. Lett.*, vol. 48, no. 1, pp. 78-80, 1986.

[8] H. Han, L. E. Weiss, and M. L. Reed, "Design and modelling of a micromechanical surface bonding system," in *Proc. Sixth Int. Conf. Solid-State Sensors and Actuators*, San Francisco, CA, 1991, pp. 974-977.

[9] S. P. Timoshenko and J. N. Goodier, *Theory of Elasticity*, 2nd ed. New York: McGraw-Hill, 1951.

[10] S. P. Timoshenko, *Strength of Materials*, 3rd ed. New York: D. Van Nostrand, 1955.

[11] T. P. Weihs, S. Hong, J. C. Bravman, and W. D. Nix, "Mechanical deflection of cantilever microbeams: A new technique for testing the mechanical properties of thin films," *J. Mater. Res.*, vol. 3, no. 5, pp. 931-942, 1988.

[12] P. P. Gillis and J. J. Gilman, "Double-cantilever mode of crack propagation," *J. Appl. Phys.*, vol. 35, no. 3, pp. 647-658, 1964.

[13] K. E. Petersen and C. R. Guarnieri, "Young's modulus measurements of thin films using micromechanics," *J. Appl. Phys.*, vol. 50, no. 11, pp. 6761-6766, 1979.

Hongtao Han (S'90) was born in Shenyang, China, on February 27, 1963. He received the B.S. degree in physics from Beijing (Peking) University, China, in 1984, and the M.S. degree in semiconductor and device physics from the Institute of Semiconductors, Academy of Sciences, China, in 1987. He is currently working toward the Ph.D. degree in the Department of Electrical and Computer Engineering at Carnegie Mellon University, developing micromechanical fastening systems incorporating micromachined silicon structures.

Mr. Han is a member of the American Physical Society.

Lee E. Weiss (M'79) received the B.S. degree in electrical engineering from the University of Pittsburgh, Pittsburgh, PA, in 1972, and the M.S. degree in bioengineering and the Ph.D. degree in electrical and computer engineering from Carnegie Mellon University, Pittsburgh, PA, in 1974 and 1984, respectively.

He is currently a Senior Research Scientist in the Robotics Institute and in the Engineering Design Research Center of Carnegie Mellon University. His research interests include thermal shape deposition technologies for rapid prototyping and tool manufacturing, and biomedical applications of micromechanisms.

Dr. Weiss is a member of ASME.

Michael L. Reed (M'80) received B.S. and M.Eng. degrees in electrical engineering from Rensselaer Polytechnic Institute, Troy, NY, and the Ph.D. degree in electrical engineering from Stanford University, Stanford, CA.

From 1980 to 1983, he was on the staff of Hewlett-Packard Laboratories, Palo Alto, CA. Since 1987, he has been on the faculty of Carnegie Mellon University, Department of Electrical and Computer Engineering, Pittsburgh, PA. His research interests include microelectromechanical systems, piezoelectrically tuned electrooptic devices, and applications of scanning tunneling potentiometry.

Dr. Reed is a recipient of a Hertz Foundation Prize, an IBM Faculty Development Award, and an NSF Presidential Young Investigator Award. He is a member the American Physical Society, Tau Beta Pi, Eta Kappa Nu, the American Society for Engineering Education, and the MEMS-92 Technical Program Committee.